

# **Machine learning thermal circuit network model for thermal design optimization of electronic circuit board layout with transient heating chips**

Daiki OTAKI<sup>1</sup>, Hirofumi NONAKA<sup>2</sup>, Noboru YAMADA<sup>1,\*</sup>

<sup>1</sup> Department of Mechanical Engineering, Nagaoka University of Technology, 1603-1, Kamitomioka,  
Nagaoka, Niigata, 940-2133

<sup>2</sup> Department of Information and Management Engineering, Nagaoka University of Technology, 1603-  
1, Kamitomioka, Nagaoka, Niigata, 940-2133

\*Corresponding author: noboru@nagaokaut.ac.jp

## **Abstract**

This paper describes a method combining Bayesian optimization (BO) and a lumped-capacitance thermal circuit network model that is effective for speeding up the thermal design optimization of an electronic circuit board layout with transient heating chips. As electronic devices have become smaller and more complex, the importance of thermal design optimization to ensure heat dissipation performance has increased. However, such thermal design optimization is difficult because it is necessary to consider various trade-offs associated with packaging and transient temperature changes of heat-generating components. This study aims to improve the performance of thermal design optimization by artificial intelligence. BO using a Gaussian process was combined with the lumped-capacitance thermal circuit network model, and its performance was verified. As a result, BO successfully found the ideal circuit board layout that particle swarm optimization (PSO) and genetic algorithm (GA) could not. The CPU time for BO was 1/20 of that for PSO and GA. In addition, BO found a non-intuitive optimal solution in approximately 7 min from 10 million layout patterns. It was estimated that this was 1/1000 of the CPU time required for analyzing all layout patterns.

*Key Words:* Bayesian optimization, Machine learning, Thermal design, Thermal circuit network model, Circuit board

## **1. Introduction**

In recent years, electronic devices and energy storage systems have become smaller (thinner), and their internal structures have become more complex; therefore, ensuring the heat dissipation performance of these devices has become an issue. Thermal design and temperature control are becoming key elements in improving product performance and reliability[1][2]. For example, temperature suppression methods combining composites, fins, fluids, and phase change materials (PCMs) amongst others, have been studied previously [3][4][5][6][7][8][9][10][11]. Most of the heat generated inside a small electronic device is dissipated through the circuit board (CB) on which the heat-generating components are mounted, and then dissipated to its surroundings. To improve this heat dissipation, i.e., cooling performance, it is necessary to optimize the layout of the heat-generating components mounted on the CB (hereinafter referred to as the CB layout). This optimization process requires consideration of trade-offs due to various constraints in product packaging and a large number of layout patterns, making the search for an optimal solution difficult. Therefore, the development of efficient thermal design methods using artificial intelligence (AI) has been reported [12][13][14][15][16][17][18][19]. Lianlian et al. [12] used ant colony optimization (ACO) to optimize the printed CB layout. However, it has been reported that ACOs tend to provide a local solution [20][21]. Ref. [12] did not compare the layout pattern obtained by ACO with the true optimum layout, so there is room for further research. Alexandridis et al. [13] applied particle swarm optimization (PSO) to a similar CB layout optimization. However, the search performance of PSO is strongly influenced by hyperparameters, and it is necessary to determine the appropriate

hyperparameters for each problem [22]. Ismail et al. [14] used a genetic algorithm (GA) for a similar CB layout optimization; however, GA has many hyperparameters that affect the search performance as seen in PSO; therefore, it is difficult to determine appropriate hyperparameters [23]. By contrast, Bayesian optimization (BO) using Gaussian processes, known as a type of machine learning, has recently been applied to achieve the optimal design of various devices and systems [24][25][26][27][28][29][30][31]. It has been reported that BO does not easily fall into a local solution [32][33], and its algorithm is provided as a programming library for ease of use. Therefore, BO may be effective for the CB layout optimization problem; however, its effectiveness has not been verified so far, to the best of the authors' knowledge.

In this study, BO is combined with a lumped-capacitance thermal circuit network model and applied to CB layout optimization problems, and its effectiveness is verified by comparing it with other algorithms (PSO and GA). Furthermore, the optimization was carried out based on unsteady state temperature simulations in which time variations of heating power and temperature of the components were taken into account. In the reported studies on CB layout optimization, the heating power of the heating components is assumed to be constant, and the layout optimization is performed using the temperature under steady-state conditions. However, in actual CBs, the heating power often varies with time.

## 2. Simulation model and problem setting

### 2.1 Thermal circuit network model for CB layout optimization

A lumped-capacitance thermal circuit network model (LTCNM) was used for the transient temperature simulation of a CB. LTCNM is a model based on the analogy between electrical circuits and heat transfer phenomena and is widely used in the design simulation of thermal systems because it allows unsteady heat transfer simulation of systems without fine computational mesh and time-consuming complex fluid simulation [34][35][36][37][38][39][40].

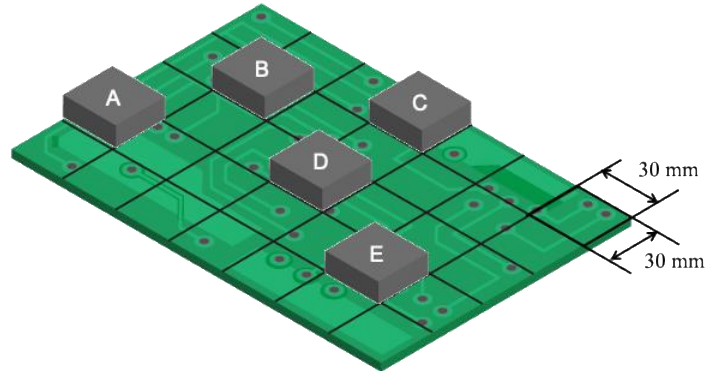


Fig. 1 Circuit board model consisting of board and five heating chips (A-E)  
(the electronic circuit pattern illustration on the board is just a texture and not considered in the simulation)

Figure 1 shows the CB model to be optimized. There are five heat-generating components (hereafter referred to as heating chips or chips) on the CB. The dimensions, maximum heating power, and integrated heating energy (for  $0 \leq t \leq 1800$  s) of the CB and each chip are summarized in Table 1.

Table 1 Specification of circuit board model components

	Dimensions [mm]	Max. heating power [W]	Integrated heating energy [Wh]
Board	$210 \times 150 \times 1$	N/A	N/A
Chip A	$30 \times 30 \times 10$	3.2	1.54
Chip B	$30 \times 30 \times 10$	3.0	1.25
Chip C	$30 \times 30 \times 10$	3.4	1.03
Chip D	$30 \times 30 \times 10$	3.0	0.83
Chip E	$30 \times 30 \times 10$	2.0	0.50

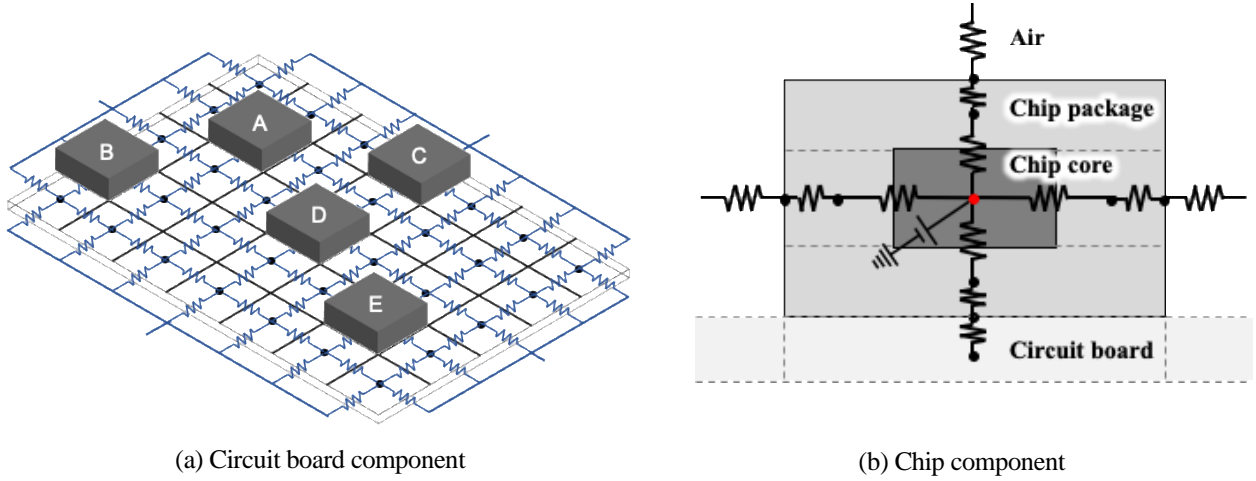


Fig. 2 Lumped-capacitance thermal circuit network model for circuit board model

Figure 2(a) shows the thermal circuit network model for the CB. The CB consists of  $5 \times 7$  computational nodes. Figure 2(b) shows the thermal circuit network model for the heating chip. It consists of a central semiconductor chip core (red-colored 1 node), which is the heat source, and its surrounding resin chip package (6 nodes). The thermophysical properties of the model components are summarized in Table 2.

Table 2 Thermophysical properties of circuit board model components

	Board	Chip package	Chip core
Materials	Aluminum	Epoxy resin	Silicon
Specific heat [J/g·K]	0.9	1.5	0.77
Density [g/cm <sup>3</sup> ]	2.7	1.2	2.3
Conductivity [W/m·K]	170	0.3	156

As shown in Fig. 3, it was assumed that the heating power of each chip varied with time. Each chip has different time-varying characteristics, and the total heating power, which is the sum of the heating power of each chip (black line), and peaks at  $t = 1047$  s.

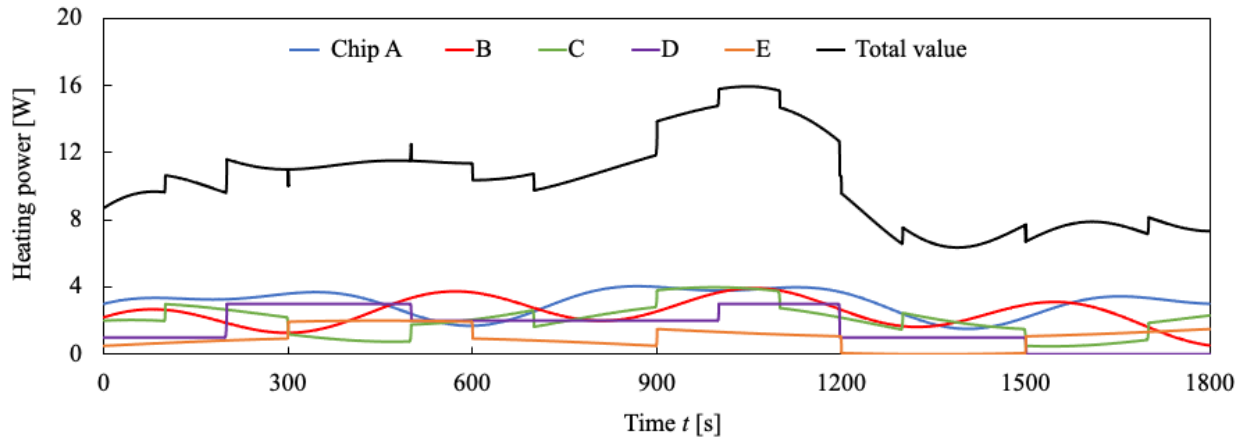


Fig. 3 Time-variations of heating power of five heating chips (A-E) in circuit board model

Because the lumped-capacitance model is used, the heat capacitance is connected to every node in Figure 2(a) and (b), although their circuit symbols are omitted in the figures. It is noted that the circuit symbols of thermal resistance between the nodes and the ambient air are also omitted. In LTCNM, the temperature at the  $n$ th node is calculated as:

$$\sum_{i=1}^l Q_i = \frac{dT_n}{dt} m_n c_n \quad (1)$$

where  $Q_i$  [W] is the amount of heat flowing from the neighboring nodes,  $l$  is the number of neighboring nodes,  $T_n$  [K] is temperature,  $t$  [s] is time,  $m_n$  [kg] is mass,  $c_n$  [J/kg·K] is the specific heat, and the subscript indicates the number of nodes.  $Q_i$  is calculated by the following equation:

$$Q_i = \frac{\Delta T_i}{R_i} \quad (2)$$

$\Delta T_i$  [K] is the temperature difference between the  $n$ th node and the adjacent node,  $R_i$  [W/K] is the thermal resistance considering conduction and convection [36]. The initial and boundary conditions are listed in Table 3. This model was implemented in MATLAB/Simulink, and an unsteady heat transfer simulation was performed to obtain the temperature change characteristics of each node. The chip temperature is defined as the average temperature over the nodes within the chip component.

Table 3 Simulation conditions

Initial temperature of all components	25 °C
Air temperature	25 °C (Constant)
Boundary conditions	Board-Air: Natural convection Chip-Air: Natural convection Board side and bottom: Adiabatic
Heat transfer Coefficient for natural convection	10 W/m <sup>2</sup> ·K

## 2.2 Optimization problem setting

The target of the optimization is the CB layout, that is, the placement pattern of five transient heating chips A to E. In actual product design, there may be restrictions on chip placement depending on the functions of the devices. To simulate this situation, two restrictions on chip placement are given as i) placeable area for each chip and ii) distance between chips. In restriction i), each chip can only be placed in a mesh defined by a frame of the same color as the color of the chip symbol, as shown in Figure 4. In other words, each chip can only be placed within a specified area. In restriction ii), the distance between the nodes at the center of the chips must be less than or equal to the values shown in Table 4. For example, in Figure 4, the distance between chips A and B is 51.96 mm, which satisfies the restricted value (90 mm).

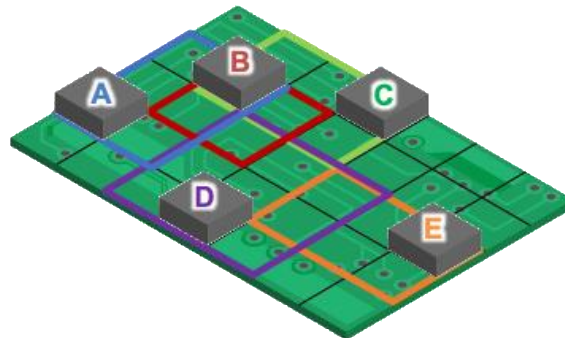


Fig. 4 Restriction i): Colored mesh depicts placeable areas for each chip with the same colored symbols

The optimization was performed so that the value of the following objective function  $f(x)$  was minimized:

$$f(x) = w \max \{T_{\text{mean}}(t)\} + (1 - w) \max \{T_{\text{high}}(t)\} \quad (3)$$

where  $x$  indicates one of the CB layouts.  $T_{\text{mean}}(t)$  is the mean chip temperature, that is, the average chip temperature over the five chips at time  $t$ ;  $T_{\text{high}}(t)$  is the highest chip temperature among the five chips at time  $t$ ;  $\max\{\}$  is the maximum value during the simulation time period ( $0 \leq t \leq 1800$  s);  $w$  is the weight coefficient; with the optimization being performed for three cases namely:  $w = 1, 0$ , and  $0.5$ . This methodology is called the weighted sum method and is commonly used for multi-objective optimization [41][42]. The objective function for  $w = 1, 0$ , and  $0.5$  is  $f(x) = \max\{T_{\text{mean}}(t)\}$ ,  $f(x) = \max\{T_{\text{high}}(t)\}$ , and  $f(x) = [\max\{T_{\text{mean}}(t)\} + \max\{T_{\text{high}}(t)\}]/2$ , respectively.

Table 4 Restriction ii)

Max. distance between the chips [mm]	
Chips A-B	90
Chips B-C	90
Chips A-D or D-E	90

### 3. Validation of the simulation model

Prior to performing the optimization and to confirm the validity of the present LTCNM, three-dimensional (3D) finite element method (FEM) simulations under the same model and conditions were conducted, and the results were compared with the results obtained by LTCNM. The commercial software ANSYS was used for the FEM simulation. FEM simulation is a widely used simulation in the field of heat transfer engineering. The FEM simulation generally provides reliable results; however, it requires a fine 3D computational mesh and a fine time step, resulting in high computational cost. The number of computational meshes used in the FEM model was set to 3630. By contrast, the number of computational nodes in LTCNM is 95. A comparison of the results from FEM and LTCNM is shown in Figures 5 and 6. The upper and bottom figures in Figures 5 (a)–(d) show the FEM and LTCNM results of temperature distribution at elapsed times  $t = 250$  s,  $750$  s,  $1250$  s, and  $1800$  s, respectively. The LTCNM results depict the mean temperature over the surface nodes within each mesh. The trends of the temperature distributions in both simulations agreed well. For a more quantitative comparison, Figure 6 shows a comparison of the time variation of chip temperature, that is, the volume average temperature of the chip component, in both simulations. The trends of each chip were consistent. These results show that the present LTCNM has sufficient validity for the CB layout optimization, although the spatial resolution of temperature distribution is lower than that of FEM simulations.

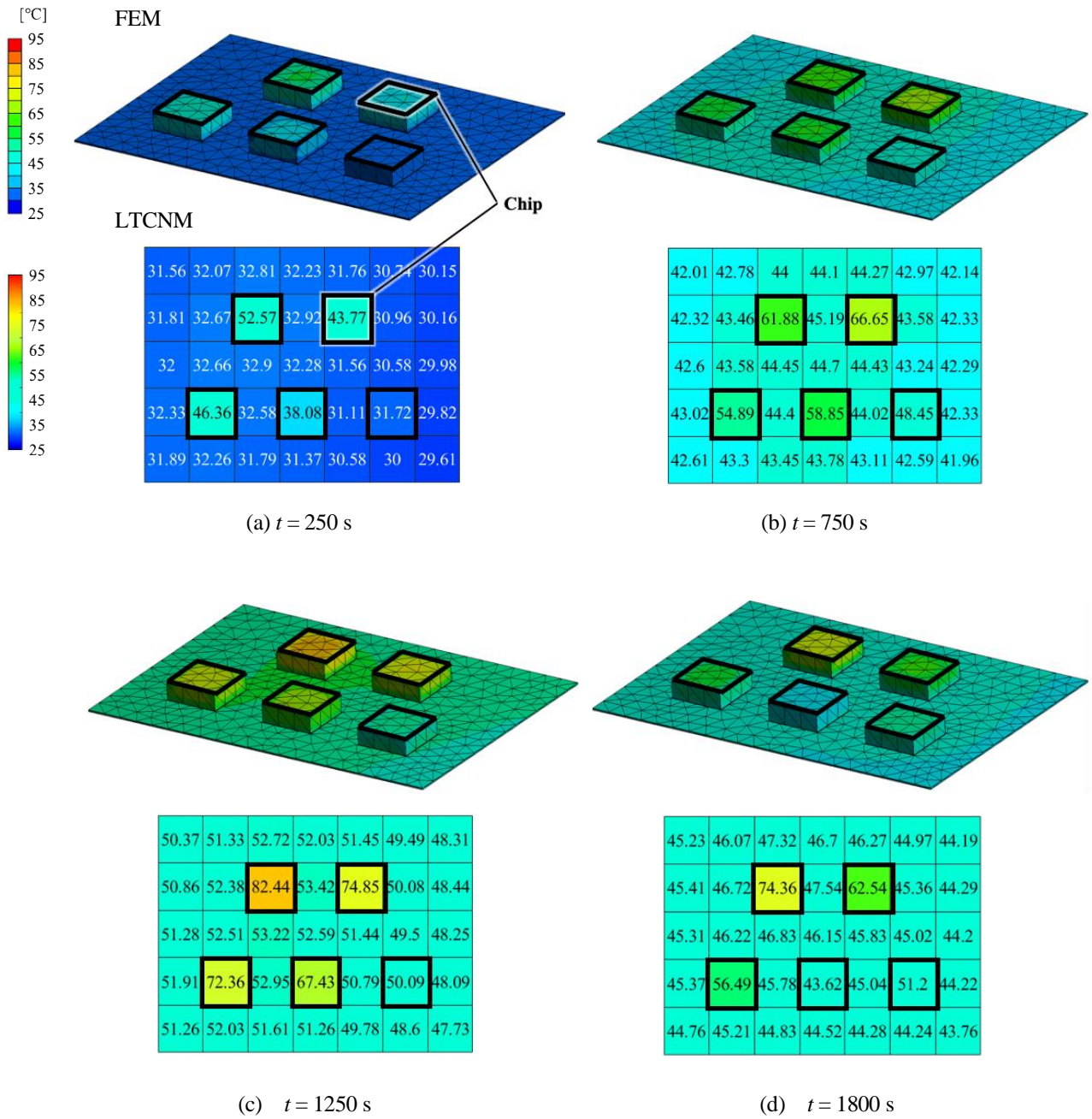


Fig. 5 Comparison of simulated temperature distributions between FEM (upper figure) and LTCNM (bottom figure) at  $t = 200$  s,  $500$  s,  $1000$  s, and  $2000$  s.

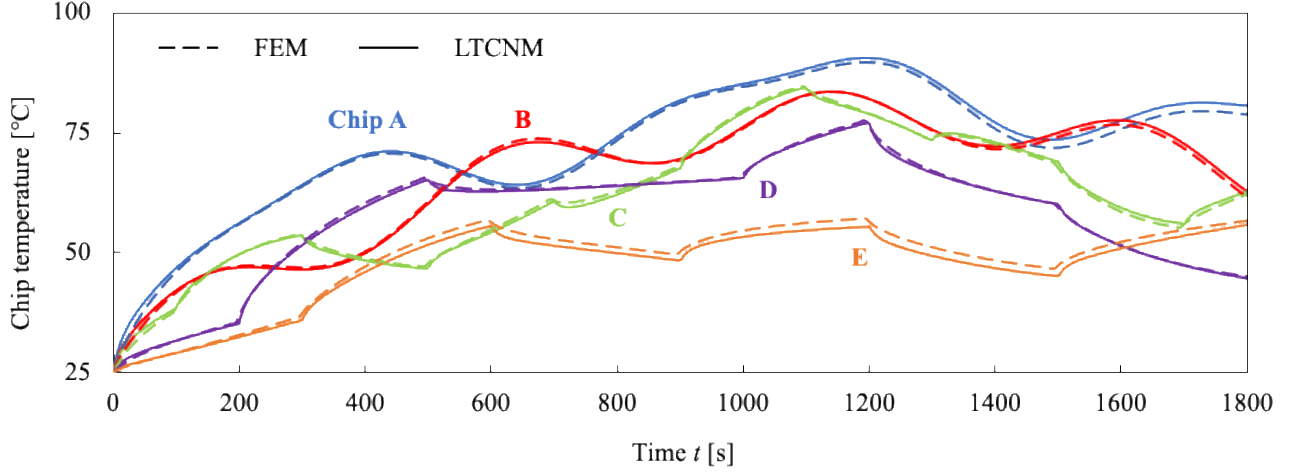


Fig. 6 Comparison of simulated chip temperature between FEM and LTCNM

#### 4. Applying Bayesian optimization

The thermal design optimization problem can be formulated as an optimization of the black box continuous functions  $f(x)$  as follows:

$$x = \operatorname{argmin}_x f(x) \quad (4)$$

where  $x$  is the input variable and  $f(x)$  denotes the objective function shown in Equation (3). The de-facto standard model for black-box optimization is the Bayesian optimization (BO) with a Gaussian process. Bayesian optimization (BO) is a popular framework for optimizing the black box function owing to its sample efficiency. The Gaussian process has been widely applied to solve real-world problems such as the prediction of thermal systems because of its ability to capture non-linearity and quantify uncertainty [43][44][45]. Due to such characteristics, a Gaussian process is often selected to model the unknown objective function of BO. In BO,  $f(x)$  is a stochastic process, which is assumed to follow a Gaussian process, that is, the following equation (5), where  $\mu(x)$  is the mean function (of the objective function at point  $x$ ),  $\sigma(x)$  is the covariance function (of the objective function at a point  $x$ ), and  $k(x, x')$  is the kernel function.

$$f(x) \sim GP(\mu(x), \sigma(x)) = GP(\mu(x), k(x, x')) \quad (5)$$

In this method, the posterior distribution of  $f(x)$  is calculated from the currently observed data based on Equation (5), and the next search point is determined using the acquisition function based on the information of the peripheralized predicted distribution. This process is repeated to find the optimal solution[46][47][48]. The Matérn5/2 kernel [33] was used as well as an expected improvement (EI) [32][33]. The combination of EI and the Matérn5/2 kernel is often used in practical applications [29]. In simulation, the “bayesopt” function of MATLAB library was used. Optimization with PSO and GA was also performed and compared with BO. The “particle swarm” and “ga” functions of the MATLAB library were used for PSO and GA, respectively. The swarm size of the PSO and the population size of the GA were set to 5 for both algorithms. The other hyperparameters used the default values of the functions. The total number of iterations was set to 200 for all algorithms. To determine the true optimal CB layout (henceforth, ideal layout), all 7776 layout patterns were searched and  $f(x)$  for them were evaluated in advance. The performance of each algorithm was verified by comparing their optimized layout with the ideal layout. The CPU time consumed by each algorithm was compared. All the simulations were conducted on a Windows workstation with AMD Ryzen9 3950X 3.49 GHz and 16 GB memory. Note that previous studies [12][13][14][15][16][17][18] have not made comparisons with the ideal layout.



## 5. Optimization results

Tables 5 and 6 show the comparison of optimization results, that is, values of  $f(x)$  of the optimized CB layout, and CPU time, for each algorithm including all layout pattern searches. With 200 iterations, BO reached the same layout as the ideal layout regardless of the  $f(x)$  case, while by contrast, PSO and GA did not reach the ideal layout regardless of the  $f(x)$  case. BO reached the ideal layout in approximately 1/25 of CPU time for all layout pattern searches, and BO completed 200 iterations in approximately 1/10 of the CPU time of PSO and GA. The swarm size and the population size affect the CPU time of PSO and GA, respectively. In this case, because both sizes are set to 5, PSO and GA must evaluate 5 layout patterns per iteration. By contrast, BO evaluated one layout pattern per iteration. As the transient temperature simulation per layout pattern takes a long CPU time, PSO and GA must take a longer CPU time per iteration than BO. This is the reason for the increase in CPU time for PSO and GA.

Table 5 Comparison of optimization results (temperature).

Objective function (Optimization to minimize $f(x)$ )	$f(x)$ of the optimized CB layout [°C]			
	Searching all layout patterns	BO	PSO	GA
$f(x) = \max\{T_{\text{mean}}(t)\}$	<b>76.88</b>	<b>76.88</b>	77.25	77.45
$f(x) = \max\{T_{\text{high}}(t)\}$	<b>90.20</b>	<b>90.20</b>	90.23	90.73
$f(x) = [\max\{T_{\text{mean}}(t)\} + \max\{T_{\text{high}}(t)\}]/2$	<b>83.68</b>	<b>83.68</b>	85.53	83.70

Table 6 Comparison of optimization results (CPU time).

Objective function (Optimization to minimize $f(x)$ )	CPU time [s]			
	Searching all layout patterns	BO	PSO	GA
$f(x) = \max\{T_{\text{mean}}(t)\}$	9836	<b>417</b>	3760	3382
$f(x) = \max\{T_{\text{high}}(t)\}$	9836	<b>434</b>	3814	3416
$f(x) = [\max\{T_{\text{mean}}(t)\} + \max\{T_{\text{high}}(t)\}]/2$	9836	<b>442</b>	3799	3412

Figure 7 shows the comparison of the optimization progress, that is, the evolution of the objective function value with respect to iterations in each algorithm. BO has been steadily updating its optimal value in three  $f(x)$  cases, and it reached an almost ideal layout in less than 100 iterations. By contrast, PSO and GA did not change their optimal values after more than 10 iterations, which suggests that they possibly fell into a local solution. This issue may be mitigated by careful tuning of hyperparameters, for example, increasing the swarm size and the population size; however, such a tuning itself is time-consuming. These results imply that BO is more efficient and faster than PSO and GA for the CB layout optimization problem, in which the computational cost per layout pattern is high owing to the transient temperature simulation.



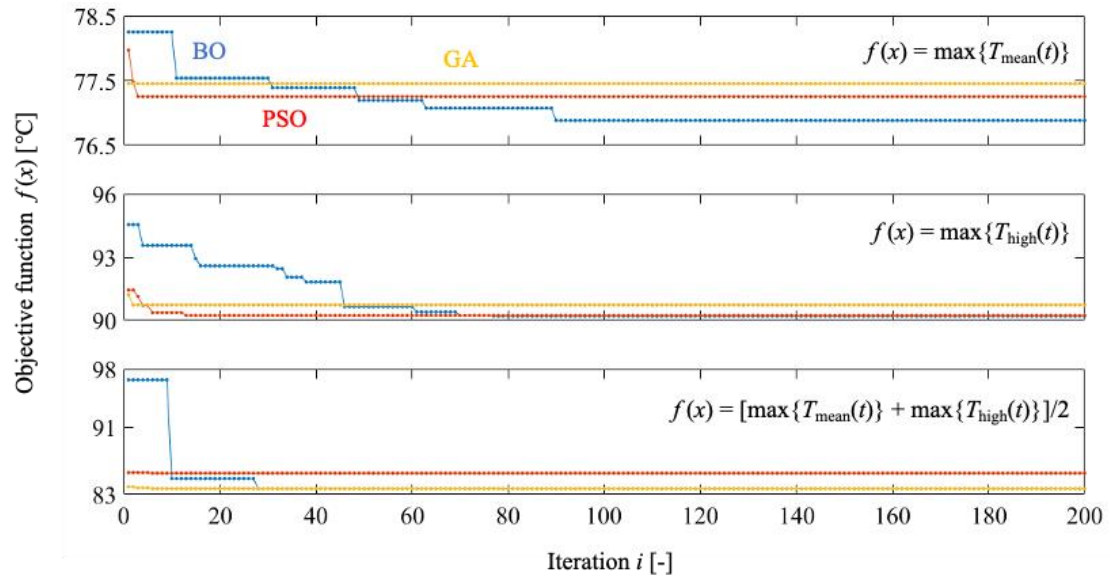
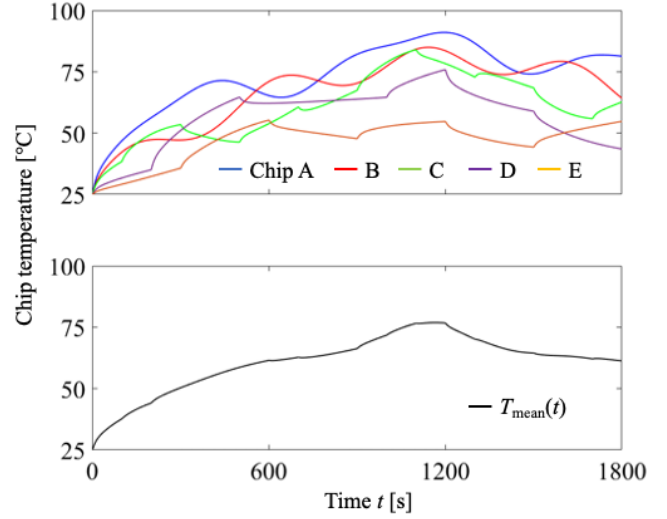
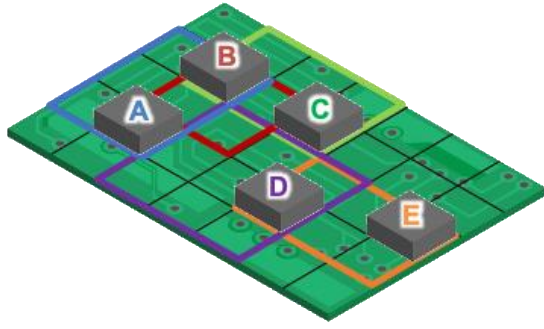
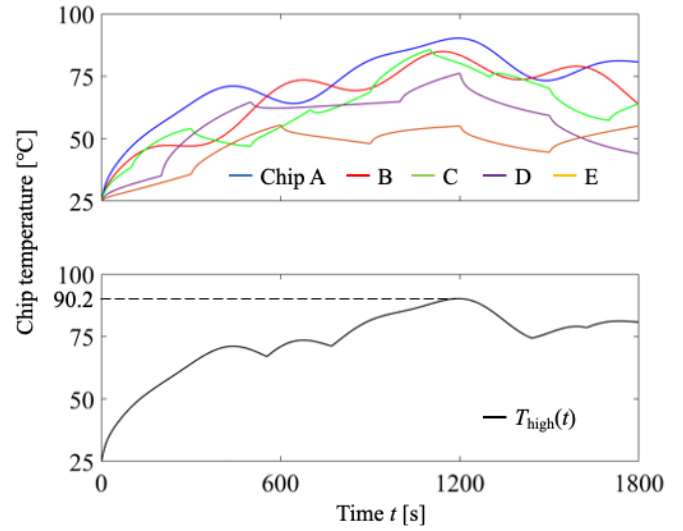
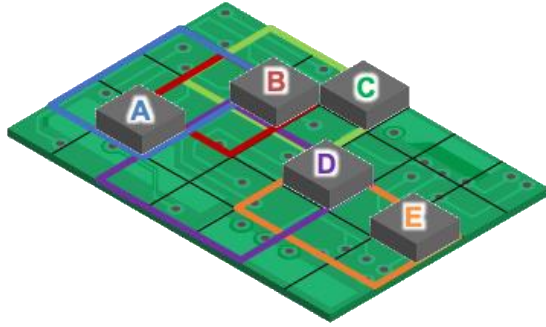


Fig. 7 Comparison of optimization progress. Variation of objective function value with respect to iterations.

Figure 8(a) and (b) show the optimized layouts (which are identical to the ideal layouts) obtained by BO in three  $f(x)$  cases, respectively. In the figures, the corresponding time variations of each chip temperature and  $T_{\text{mean}}(t)$  or  $T_{\text{high}}(t)$  are also shown. In Fig. 8(a),  $T_{\text{mean}}(t)$  reaches the maximum value at approximately  $t = 1200$  s. This maximum value is the temperature of Chip A, which has the highest total heat generation, as shown in Table 1. In this case, because the chips should be evenly distancing to minimize  $f(x) = \max\{T_{\text{mean}}(t)\}$ , it would be easy for us to predict a similar layout pattern intuitively. By contrast, in Fig. 8(b), with the optimization to minimize  $f(x) = \max\{T_{\text{high}}(t)\}$ , Chips B and C are arranged close to each other, and Chip A is mostly distancing from the other chips, which would not be easy for us to predict intuitively. This indicates that the optimized layouts are reasonable and that the thermal design optimization using BO, that is, a type of machine learning, is effective.



(a)  $f(x) = \max\{T_{\text{mean}}(t)\}$



(b)  $f(x) = \max\{T_{\text{high}}(t)\}$

Fig. 8 Comparison of optimized component layouts by BO for different objective functions.

## 6. Applying BO to extended problem settings

In the actual thermal design of CBs, the number of layout patterns can be even greater. To test the performance of BO in such a case, BO was applied to an extended problem setting in which the restrictions i) and ii) described in section 2.2 are removed. In this case, the number of possible layout patterns is approximately 10 million. The optimization for  $f(x) = \max\{T_{\text{high}}(t)\}$  case was performed. Figure 9 shows the evolution of the value of the objective function with respect to the number of iterations. The values of  $f(x)$  at the 20, 200, and 2000 iterations are shown in the graph. Figure 10 shows the corresponding optimized layouts and the time variations of the chip temperature and  $T_{\text{high}}(t)$  for the optimized layout at 2000 iterations. From Figure 9, the value of  $f(x)$  is updated as the number of iterations increases, reaching 90% of the 2000 iterations' value at 200 iterations.  $T_{\text{high}}$  at 200 and 2000 iterations were reduced by 2.79°C and 2.9°C, respectively, compared to the  $T_{\text{high}}$  (90.20°C) under restrictions i) and ii), as shown in Table 5 in Chapter 5. Figure 10 shows that Chips A and B were optimized to maintain distance from the other chips. This is because the heating power of Chips A and B is relatively larger, as shown in Table 1, so they are placed farther distancing from each other to lower  $T_{\text{high}}$ . Comparing the temperature trends in Fig. 10(c) and Fig. 8(b), the temperature of Chip A decreases. The CPU times for 200 and 2000 iterations were 434 s and 16676 s, respectively. Based on the results in Chapter 5, the estimated CPU times for 2000 iterations for PSO and GA are 35,000 s, which is approximately 2.1 times longer than that of BO. Similarly, the CPU time required for the simulation of all layout patterns search was estimated

to be about 140 days, and BO was able to optimize at approximately 1/1000 of the time for all layout pattern searches. From these results, the high speed of BO was confirmed in the extended problem setting. However, it is reported that the computational complexity of BO tends to increase with the number of iterations [48]. This fact was also confirmed by the present result. The CPU time for 2000 iterations was 38 times higher than that for 200 iterations. This characteristic should be considered when performing the optimization by BO.

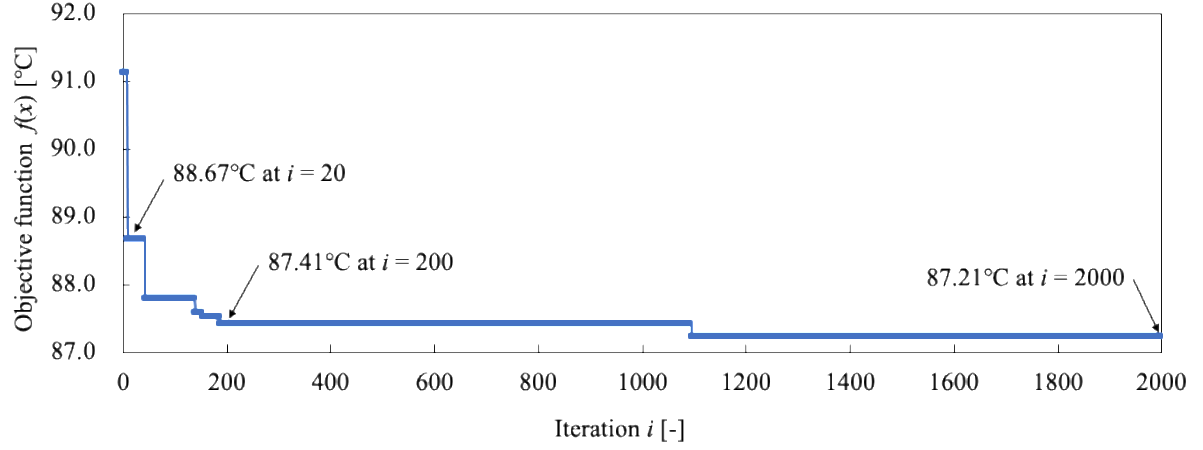
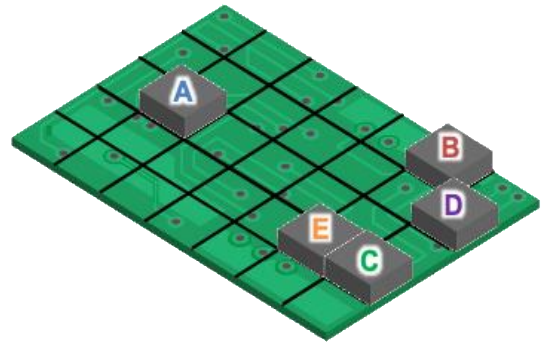


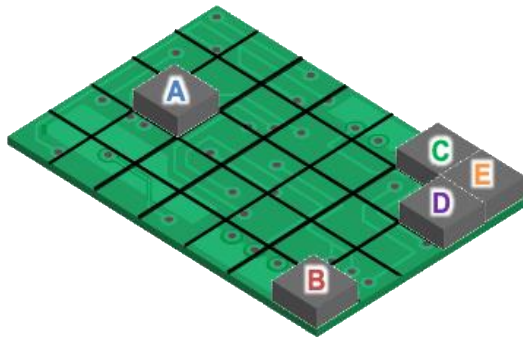
Fig. 9 Optimization progress by BO



(a)  $i=20$



(b)  $i=200$



(c)  $i=2000$

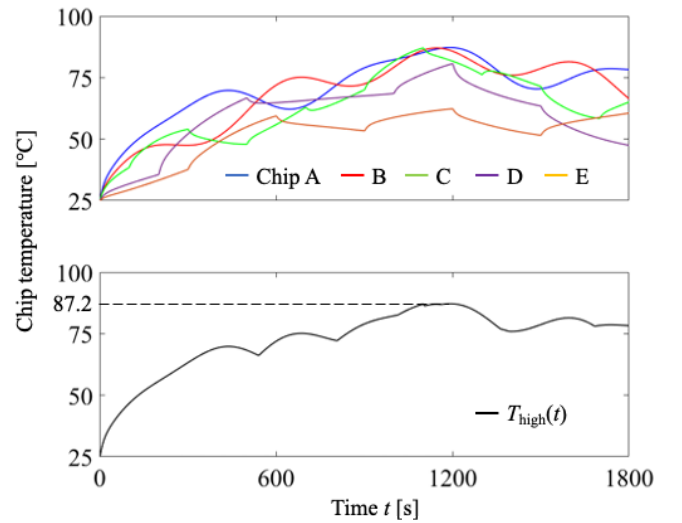


Fig. 10 Optimized component placement by BO w/o restrictions i) and ii).

## 7. Conclusion

The lamped-capacitance thermal circuit network model combined with BO was applied to the layout optimization of an electronic circuit board with transient heating chips, and its effectiveness was verified by fundamental case studies. To evaluate the value of the objective function of the examined layout, a transient heat transfer simulation was performed per layout taking into account the different temporal variations of the heating power of the heat-generating chips. As a result, BO found the ideal layout in 1/25 CPU time for all layout pattern searches. By contrast, for the same optimization problem, PSO and GA could not find the ideal layout even though they required 10 times as much CPU time to simulate the same number of iterations as BO. Furthermore, BO was applied to the extended problem setting with possible layout patterns of 10 million. BO found a reasonably best layout, which achieved 90% of the objective function value of 2000 iterations, at 200 iterations. It took only approximately 7 min. All layout pattern searches would have required 140 days, and BO took only 1/1000 of that time for optimization. In addition, by comparing it with other algorithms (PSO and GA), the effectiveness of the present method (lamped-capacitance thermal circuit network model + BO) was confirmed for the CB layout optimization problem that requires a transient heat transfer simulation. In future research, it will be necessary to upgrade to a more realistic model that also considers more complicated circuit board structures and conditions.

## References

- [1] S. V. Garimella, T. Persoons, J. A. Weibel, and V. Gektin, "Electronics Thermal Management in Information and Communications Technologies: Challenges and Future Directions," *IEEE Trans. Components, Packag. Manuf. Technol.*, vol. 7, no. 8, pp. 1191–1205, 2017, doi: 10.1109/TCPMT.2016.2603600.
- [2] T. Dbouk, "A review about the engineering design of optimal heat transfer systems using topology optimization," *Appl. Therm. Eng.*, vol. 112, pp. 841–854, 2017, doi: 10.1016/j.applthermaleng.2016.10.134.
- [3] B. Ding, Z. H. Zhang, L. Gong, M. H. Xu, and Z. Q. Huang, "A novel thermal management scheme for 3D-IC chips with multi-cores and high power density," *Appl. Therm. Eng.*, vol. 168, no. July 2019, p. 114832, 2020, doi: 10.1016/j.applthermaleng.2019.114832.
- [4] Z. Sun, R. Fan, F. Yan, T. Zhou, and N. Zheng, "Thermal management of the lithium-ion battery by the composite PCM-Fin structures," *Int. J. Heat Mass Transf.*, vol. 145, p. 118739, 2019, doi: 10.1016/j.ijheatmasstransfer.2019.118739.
- [5] Y. Lai, W. Wu, K. Chen, S. Wang, and C. Xin, "A compact and lightweight liquid-cooled thermal management solution for cylindrical lithium-ion power battery pack," *Int. J. Heat Mass Transf.*, vol. 144, p. 118581, 2019, doi: 10.1016/j.ijheatmasstransfer.2019.118581.
- [6] Q. Ren, P. Guo, and J. Zhu, "Thermal management of electronic devices using pin-fin based cascade microencapsulated PCM/expanded graphite composite," *Int. J. Heat Mass Transf.*, vol. 149, pp. 1–16, 2020, doi: 10.1016/j.ijheatmasstransfer.2019.119199.
- [7] W. G. Alshaer, S. A. Nada, M. A. Rady, E. P. Del Barrio, and A. Sommer, "Thermal management of electronic devices using carbon foam and PCM/nano-composite," *Int. J. Therm. Sci.*, vol. 89, pp. 79–86, 2015, doi: 10.1016/j.ijthermalsci.2014.10.012.
- [8] C. Qian *et al.*, "Thermal Management on IGBT Power Electronic Devices and Modules," *IEEE Access*, vol. 6, pp. 12868–12884, 2018, doi: 10.1109/ACCESS.2018.2793300.
- [9] S. Kumar, "Thermal Management of RF and Digital Electronic Assemblies using Optimized Materials and PCB Designs," *MILAERO007-Military Aersp. Electron. news Inf.*, 2012.
- [10] A. L. Moore and L. Shi, "Emerging challenges and materials for thermal management of electronics," *Mater. Today*, vol. 17, no. 4, pp. 163–174, 2014, doi: 10.1016/j.mattod.2014.04.003.
- [11] M. Andresen and M. Liserre, "Impact of active thermal management on power electronics design," *Microelectron. Reliab.*, vol. 54, no. 9–10, pp. 1935–1939, 2014, doi: 10.1016/j.microrel.2014.07.069.

- [12] L. Wang, G. Lu, and K. Yang, "Thermal optimization of electronic devices on PCB based on the ant colony algorithm," *2018 Int. Conf. Electron. Technol. ICET 2018*, pp. 55–59, 2018, doi: 10.1109/ELTECH.2018.8401424.
- [13] A. Alexandridis, E. Paizis, E. Chondrodima, and M. Stogiannos, "A particle swarm optimization approach in printed circuit board thermal design," *Integr. Comput. Aided. Eng.*, vol. 24, no. 2, pp. 143–155, 2017, doi: 10.3233/ICA-160536.
- [14] F. S. Ismail, R. Yusof, and M. Khalid, "Optimization of electronics component placement design on PCB using self organizing genetic algorithm (SOGA)," *J. Intell. Manuf.*, vol. 23, no. 3, pp. 883–895, 2012, doi: 10.1007/s10845-010-0444-x.
- [15] H. Y. Lin, C. J. Lin, and M. L. Huang, "Optimization of printed circuit board component placement using an efficient hybrid genetic algorithm," *Appl. Intell.*, vol. 45, no. 3, pp. 622–637, 2016, doi: 10.1007/s10489-016-0775-1.
- [16] Y. Satomi, K. Hachiya, T. Kanamoto, R. Watanabe, and A. Kurokawa, "Thermal placement on PCB of components including 3D ICs," *IEICE Electron. Express*, vol. 17, no. 3, pp. 20190737–20190737, 2020, doi: 10.1587/elex.17.20190737.
- [17] S. S. Liu, R. Luo, S. Aroonsantidecha, C. Chin, and H. Chen, "Fast Thermal Aware Placement With Accurate Thermal Analysis Based on Green Function," *EEE Trans. Very Large Scale Integr. Syst.*, vol. 22, no. 6, pp. 1404–1415, 2013.
- [18] Y. Y. Changqing Xu, Yi Liu, Zhangming Zhu, "An efficient energy and thermal-aware mapping for regular Network on Chip," *Proc. IEEE Comput. Soc. Annu. Symp. VLSI, ISVLSI*, no. 2014, pp. 344–349, 2014, doi: 10.1109/ISVLSI.2014.64.
- [19] C. M. Hsu, "PCB design improvement in the circuit between the north bridge and SDRAM through an integrated procedure," *Expert Syst. Appl.*, vol. 37, no. 4, pp. 2978–2990, 2010, doi: 10.1016/j.eswa.2009.09.035.
- [20] X. Wen, M. Huang, and J. Shi, "Study on resources scheduling based on ACO algorithm and PSO algorithm in cloud computing," *Proc. - 11th Int. Symp. Distrib. Comput. Appl. to Business, Eng. Sci. DCABES 2012*, vol. 1, no. 6, pp. 219–222, 2012, doi: 10.1109/DCABES.2012.63.
- [21] S. Shimomura, H. Matsushita, and Y. Nishio, "Ant Colony Optimization using Genetic Information for TSP," *Inf. Commun. Eng.*, no. 1, pp. 48–51, 2011.
- [22] M. Erik, H. Pedersen, and M. E. H. Pedersen, "Good parameters for particle swarm optimization," *Tech. Rep. HL1001, Hvass Lab.*, vol. HL1001, pp. 1–12, 2010.
- [23] I. S. Oh, J. S. Lee, and B. R. Moon, "Hybrid genetic algorithms for feature selection," *IEEE Trans. Pattern Anal. Mach. Intell.*, vol. 26, no. 11, pp. 1424–1437, 2004, doi: 10.1109/TPAMI.2004.105.
- [24] S. J. Park, B. Bae, J. Kim, and M. Swaminathan, "Application of machine learning for optimization of 3-D integrated circuits and systems," *IEEE Trans. Very Large Scale Integr. Syst.*, vol. 25, no. 6, pp. 1856–1865, 2017, doi: 10.1109/TVLSI.2017.2656843.
- [25] H. M. Torun, M. Swaminathan, A. Kavungal Davis, and M. L. F. Bellaredj, "A Global Bayesian Optimization Algorithm and Its Application to Integrated System Design," *IEEE Trans. Very Large Scale Integr. Syst.*, vol. 26, no. 4, pp. 792–802, 2018, doi: 10.1109/TVLSI.2017.2784783.
- [26] R. Campet, P. T. Roy, B. Cuenot, É. Riber, and J. C. Jouhaud, "Design optimization of an heat exchanger using Gaussian process," *Int. J. Heat Mass Transf.*, vol. 150, p. 119264, 2020, doi: 10.1016/j.ijheatmasstransfer.2019.119264.
- [27] Y. Chen *et al.*, "Bayesian Optimization in AlphaGo," *arXiv Prepr. arXiv1812.06855*, 2018.
- [28] A. Sakurai *et al.*, "Ultrathin-Band Wavelength-Selective Thermal Emission with Aperiodic Multilayered Metamaterials Designed by Bayesian Optimization," *ACS Cent. Sci.*, vol. 5, no. 2, pp. 319–326, 2019, doi: 10.1021/acscentsci.8b00802.
- [29] M. Lisicki, W. Lubitz, and G. W. Taylor, "Optimal design and operation of Archimedes screw turbines using Bayesian optimization," *Appl. Energy*, vol. 183, pp. 1404–1417, 2016, doi: 10.1016/j.apenergy.2016.09.084.

- [30] A. Tran, J. Sun, J. M. Furlan, K. V. Pagalthivarthi, R. J. Visintainer, and Y. Wang, "pBO-2GP-3B: A batch parallel known/unknown constrained Bayesian optimization with feasibility classification and its applications in computational fluid dynamics," *Comput. Methods Appl. Mech. Eng.*, vol. 347, pp. 827–852, 2019, doi: 10.1016/j.cma.2018.12.033.
- [31] M. Yin, A. Yazdani, and G. E. Karniadakis, "One-dimensional modeling of fractional flow reserve in coronary artery disease: Uncertainty quantification and Bayesian optimization," *Comput. Methods Appl. Mech. Eng.*, vol. 353, pp. 66–85, 2019, doi: 10.1016/j.cma.2019.05.005.
- [32] P. I. Frazier, "A Tutorial on Bayesian Optimization," *arXiv Prepr. arXiv1807.02811*, 2018.
- [33] C. Jeffery, "Practical Bayesian Optimization of Machine Learning Algorithms," *Relig. Arts*, vol. 17, no. 1–2, pp. 57–73, 2013, doi: 10.1163/15685292-12341254.
- [34] C. J. Ho, C. S. Huang, and R. Viskanta, "A thermal circuit model consistent with integral energy balance for internal forced convection in a circular tube," *Int. J. Heat Mass Transf.*, vol. 87, pp. 409–417, 2015, doi: 10.1016/j.ijheatmasstransfer.2015.04.030.
- [35] S. Y. Zhao and Q. Chen, "A thermal circuit method for analysis and optimization of heat exchangers with consideration of fluid property variation," *Int. J. Heat Mass Transf.*, vol. 99, pp. 209–218, 2016, doi: 10.1016/j.ijheatmasstransfer.2016.03.124.
- [36] H. Wang and H. Wang, "An analytical circuit based nonlinear thermal model for capacitor banks," *Microelectron. Reliab.*, vol. 88–90, no. June, pp. 524–527, 2018, doi: 10.1016/j.microrel.2018.06.112.
- [37] Y. Gan, J. Wang, J. Liang, Z. Huang, and M. Hu, "Development of thermal equivalent circuit model of heat pipe-based thermal management system for a battery module with cylindrical cells," *Appl. Therm. Eng.*, vol. 164, no. July 2019, p. 114523, 2020, doi: 10.1016/j.applthermaleng.2019.114523.
- [38] L. Ramotar, G. L. Rohrauer, R. Filion, and K. MacDonald, "Experimental verification of a thermal equivalent circuit dynamic model on an extended range electric vehicle battery pack," *J. Power Sources*, vol. 343, pp. 383–394, 2017, doi: 10.1016/j.jpowsour.2017.01.040.
- [39] R. Mahamud and C. Park, "Spatial-resolution, lumped-capacitance thermal model for cylindrical Li-ion batteries under high Biot number conditions," *Appl. Math. Model.*, vol. 37, no. 5, pp. 2787–2801, 2013, doi: 10.1016/j.apm.2012.06.023.
- [40] T. Bragatto, M. Cresta, F. M. Gatta, A. Geri, M. Maccioni, and M. Paulucci, "Underground MV power cable joints: A nonlinear thermal circuit model and its experimental validation," *Electr. Power Syst. Res.*, vol. 149, pp. 190–197, 2017, doi: 10.1016/j.epsr.2017.04.030.
- [41] R. T. Marler and J. S. Arora, "Survey of multi-objective optimization methods for engineering," *Struct. Multidiscip. Optim.*, vol. 26, no. 6, pp. 369–395, 2004, doi: 10.1007/s00158-003-0368-6.
- [42] M. T. M. Emmerich and A. H. Deutz, "A tutorial on multiobjective optimization: fundamentals and evolutionary methods," *Nat. Comput.*, vol. 17, no. 3, pp. 585–609, 2018, doi: 10.1007/s11047-018-9685-y.
- [43] S. Anitha Kumari and S. Srinivasan, "Ash fouling monitoring and soot-blow optimization for reheater in thermal power plant," *Appl. Therm. Eng.*, vol. 149, no. December 2018, pp. 62–72, 2019, doi: 10.1016/j.applthermaleng.2018.12.031.
- [44] Q. Zhou, Y. Wang, S. K. Choi, L. Cao, and Z. Gao, "Robust optimization for reducing welding-induced angular distortion in fiber laser keyhole welding under process parameter uncertainty," *Appl. Therm. Eng.*, vol. 129, pp. 893–906, 2018, doi: 10.1016/j.applthermaleng.2017.10.081.
- [45] Y. Lv, X. Yang, and G. Zhang, "Durability of phase-change-material module and its relieving effect on battery deterioration during long-term cycles," *Appl. Therm. Eng.*, vol. 179, no. November 2019, p. 115747, 2020, doi: 10.1016/j.applthermaleng.2020.115747.
- [46] I. Dewancker, M. McCourt, and S. Clark, "Bayesian Optimization for Machine Learning : A Practical Guidebook," *arXiv Prepr. arXiv1612.04858*, 2016.

- [47] M. Pelikan, D. E. Goldberg, and E. Cant, "BOA : The Bayesian Optimization Algorithm," *Proc. Genet. Evol. Comput. Conf. GECCO-99.*, vol. Vol. 1, pp. 525–532, 1989.
- [48] B. Shahriari, K. Swersky, Z. Wang, R. P. Adams, and N. De Freitas, "Taking the human out of the loop: A review of Bayesian optimization," *Proc. IEEE*, vol. 104, no. 1, pp. 148–175, 2016, doi: 10.1109/JPROC.2015.2494218.